Key Engineering Materials Vols. 245-246 (2003) pp. 87-94
online at http://www.scientific.net

A Strain-flexibility-based Approach to Damage Location

Daniele Zonta[1], Alessandro Lanaro[2] and Paolo Zanon[3]

[1] DIMS, University of Trento, Via Mesiano, 77, 38050 Trento, Italy, dzonta@ing.unitn.it

[2] DIMS, University of Trento, Via Mesiano, 77, 38050 Trento, Italy, alessandro.lanaro@ing.unitn.it

[3] DIMS, University of Trento, Via Mesiano, 77, 38050 Trento, Italy, paolo.zanon@ing.unitn.it

Keywords: damage location, strain-mode-shapes; flexibility matrix; civil structures.

Abstract. The effectiveness of mode-shape-based damage location methods is investigated, with specific regards to their application to the assessment of civil structures. Different location approaches proposed in the literature are compared and theoretically analysed. It is observed that, when damage is modelled as a loss in stiffness, the most direct way of exploiting mode-shapes information consists of estimating the flexibility matrix in a strain coordinate system. This matrix, referred to as strain-flexibility matrix, can be easily computed from the natural frequencies and the mode shapes expressed in terms of strain. Each diagonal element of the strain-flexibility matrix represents a local flexibility, thus changes in these quantities can be directly utilised as damage indexes. These findings have been validated through numerical and experimental examples. More specifically, the newly proposed damage indexes have been employed in the structural assessment of a 42.0 m long single-span steel bridge. The strain-flexibility indexes have been calculated comparing the experimental dynamic response, measured at 30 different locations, with that predicted through a simple FE model, representing the structure in the undamaged situation. Outcomes are consistent with the visual evidence of damage and with the outcomes of a static load test.

Introduction

Vibration based assessment methods aim at detecting, locating and quantifying the presence of structural damage, utilising specific features of the dynamic response [1]. These features include changes in the classical modal parameters (frequencies, mode shapes and damping ratios) as well as the appearance of anomalies, non-linearity and dispersion phenomena. Despite the recent increase in the scientific literature dealing with new damage identification methods, it is commonly recognized that only methods that utilise mode-shape information are proven to be effective in practical applications to civil structures. It is worth remarking that the bare comparison of the modal shapes of a structure in the undamaged and damaged situations usually do not yield useful results for damage location; indeed, the mode-shape information needs to be rearranged in a more appropriate form. The most common approaches proposed in the literature are based on concepts such as *strain mode shape*, *strain energy* and *flexibility matrix*.

Strain-mode-shape based approach. In 1991 Pandey et al. [2] demonstrated that, for a beam-like structure, a local loss of stiffness is correlated to a sensible local change in the curvature mode shapes; thus, changes in the modal curvature are worthy of being utilised as damage indexes. In the same years, Yao et al. [3] proposed to locate the damage on a steel frame by directly monitoring the Strain Frequency Response Function (SFRF) of each element, thus introducing for the first time the concept of Strain Mode Shape (SMS). Maeck and De Roeck have extensively applied SMS-based methods for assessing civil structures, and developed an original technique, based on a direct stiffness derivation from measured modal displacement derivatives, such as modal curvatures and torsion rates [4]. SMS-based methods typically utilise the information derived from a single mode shape, and they do not make use of an explicit damage model, even if their employment understood that damage is such as to cause a local loss in stiffness, affecting the local strain response.

Strain-energy-based approach. An alternate application of the strain concept to damage detection was proposed in 1995 by Stubbs et al. [5]. Within this approach, the damage is modelled as a local loss in stiffness, and the modal-strain-energy is assumed to remain the same before and after the damaging episode. Hence, given the *i*-th mode shape $\boldsymbol{\phi}_i$, the rate between the material stiffness properties E_j and E_j^* of the undamaged and the damaged *j*-th element, can be evaluated as:

$$\beta_{ji} = \frac{E_j}{E_j^*} = \frac{\boldsymbol{\phi}_i^{*T}\mathbf{K}_{j0}\boldsymbol{\phi}_i^*}{\boldsymbol{\phi}_i^{T}\mathbf{K}_{j0}\boldsymbol{\phi}_i}\frac{k_i}{k_i^*} \tag{1}$$

where k_i is the *i*-th modal stiffness, and $\mathbf{K}_{j0}$ is the contribution of the geometrical characteristics of the *j*-th member to the stiffness matrix, and the star refers to quantities in the damaged situation. If several mode shapes are used, a formulation for combining the different damage indexes β_{ij} is proposed. The matrix is the same in the undamaged and damaged situations and requires the definition of a structural model.

Flexibility-based approach. In 1994, Pandey and Biswas [6] proposed to perform damage detection directly utilizing changes in the measured flexibility matrix $\boldsymbol{\alpha}$ (i.e. the inverse of the stiffness matrix). This matrix can be obtained by starting from the modal parameters, as follows:

$$\boldsymbol{\alpha} = \boldsymbol{\Phi}\boldsymbol{\Omega}^{-1}\boldsymbol{\Phi}^T \tag{2}$$

where $\boldsymbol{\Phi}$ is the modal matrix and $\boldsymbol{\Omega}$ is the diagonal matrix containing the system eigenvectors ω_i^2 on its diagonal. Eq. 2 is generally approximated, due to the fact that the number of modes, which are known, is typically lower than the number of Degrees of Freedom (DoFs) considered. With respect to other methods, the flexibility matrix approach takes into account in a rational way the contribution of all of the measured mode shapes. The authors proposed to calculate the damage index, for each potential damage position, as the maximum absolute variation in the corresponding column. In 2002, Lu et al. [7] proposed a method, labelled *flexibility curvature*, which utilises the second derivative of the vector collecting the diagonal elements of the flexibility matrix as damage indexes.

Introducing the strain-flexibility based approach. Zonta et al. [8] observed that a coordinate system, in which strains are defined, is such that the stiffness matrix, and consequently the corresponding flexibility matrix $\boldsymbol{\alpha}'$, are diagonal. This observation suggests reformulating Eq. 2 in a more convenient manner, utilizing a strain-mode-shape set $\boldsymbol{\Phi}'$ instead of the displacement modal matrix $\boldsymbol{\Phi}$:

$$\boldsymbol{\alpha}'_{\text{diag}} = \boldsymbol{\Phi}'\boldsymbol{\Omega}^{-1}\boldsymbol{\Phi}'^T \tag{3}$$

Each diagonal element of the strain-flexibility matrix actually represents the local flexibility, thus changes in these quantities can be directly utilized as damage indexes. When damage is modelled as a loss in stiffness, the strain-flexibility matrix evaluation theoretically represents the most direct way of exploiting mode-shapes information. In the case of a beam-like structure, the strain mode shapes are typically curvatures $\boldsymbol{\phi}_i''$ and torsion rates $\boldsymbol{\phi}_i'$, and can be directly calculated from the measured mode shapes, using a central difference scheme, of the type:

$$\phi''_{j,i} = \frac{\phi_{j-1,i} - 2\phi_{j,i} + \phi_{j+1,i}}{h^2}; \qquad \phi'_{j+1/2,i} = \frac{\phi_{j+1,i} - \phi_{j-1,i}}{h} \tag{4 a,b}$$

where $\phi_{q,i}$ is the *j*-th element of the *i*-th modal vector, *h* is the longitudinal dimension of an element.

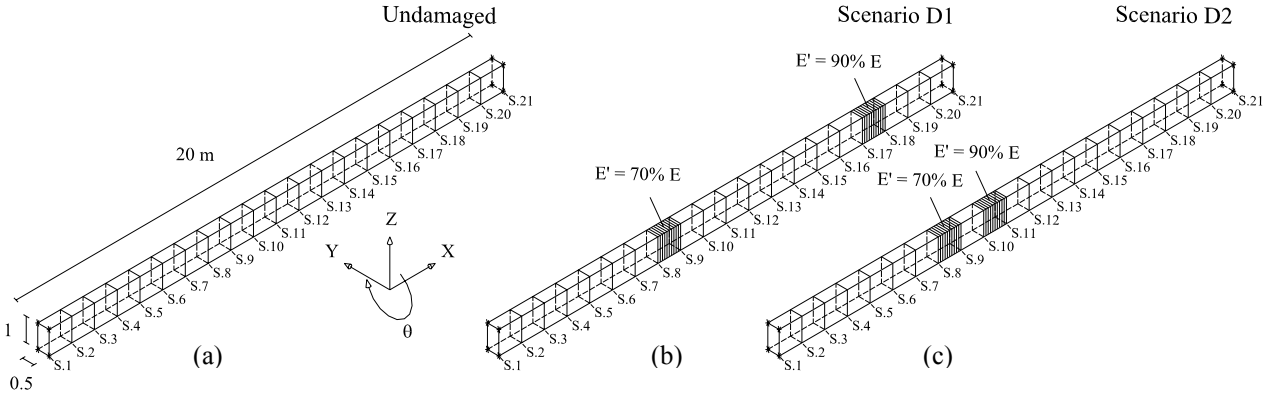

Figure 1: (a) Model, (b) damage scenario D1 and (c) damage scenario D2.

Numerical validation

The sensitivity of the newly introduced damage indexes has been numerically tested on a 3-dimensional model of a 20 m long beam, with constant rectangular section of dimensions 1.0 m by 0.5 m. In the undamaged situation, the structure has been assumed to be made of a liner elastic homogeneous material, with elastic modulus E_0=24.8 GPa, Poisson's ratio ν=0.2 and mass density ρ=2400kg m^{-3}. The beam has been divided into 20 elements, where the potential damage has been modelled as loss in the elastic modulus E.

The dynamic response of the beam has been analysed for different boundary conditions as well as for various damage locations and severities. For each case, damage has been evaluated through the following indexes: (1) the absolute change in the strain-mode-shapes, (2) the maximum absolute change in the flexibility matrix columns, (3) the percentage change in the flexibility matrix diagonal elements and (4) the percentage change in the strain-flexibility matrix diagonal element. In this paper the results relative to a fixed-end beam in the two different damage configurations shown in Fig. 1 are reported. The modal parameters of the beam in the undamaged situation are summarised in Table 1, while Fig. 2 graphically represents the outcomes of the location analyses.

Scenario D1. This damage scenario simulates a 30% reduction of E at the 8th element and a 10% reduction at the 17th element (Fig. 1(b)). All the damage indexes clearly point out the presence of an anomaly about sections S8 and S9. The light damage between sections S17 and S18 can be barely recognized utilising the strain-mode-shapes and the flexibility matrix methods. The variation in the strain-flexibility matrix diagonal elements allows locating both of the damage in a very clear manner.

Scenario D2. The second damage scenario consists of a 30% and a 10% losses in stiffness at the 8th and 10th elements, respectively (Fig. 1(c)). Since the two damaged locations are very close, most of the detection methods evidence only the main damage (S8-S9) which hides the effects of the lighter one (S10-S11). Specifically, methods based on the displacement-flexibility matrix are incapable of resolving the two damages as evidenced in Figs. 2(f) and 2(h). Conversely, the diagram of Fig. 2(j), which represents the changes in the diagonal elements of the strain-flexibility matrix, clearly point out the presence of a stiffness reduction at both of the locations. This is particularly clear in the curve relative to the elements corresponding to the torsional DoFs.

Mode	Frequency [Hz]	Mode recognition	Mode	Frequency [Hz]	Mode recognition
1	6.83	1st horizontal flexional	6	36.31	3rd horizontal flexional
2	9.86	1st vertical flexional	7	48.62	2nd torsional
3	18.69	2nd horizontal flexional	8	50.34	3rd vertical flexional
4	24.34	1st torsional	9	59.31	4th horizontal flexional
5	26.52	2nd vertical flexional	10	72.78	3rd torsional

Table 1: Natural frequencies and mode shapes of the undamaged beam.

Scenario D1 *Scenario D2*

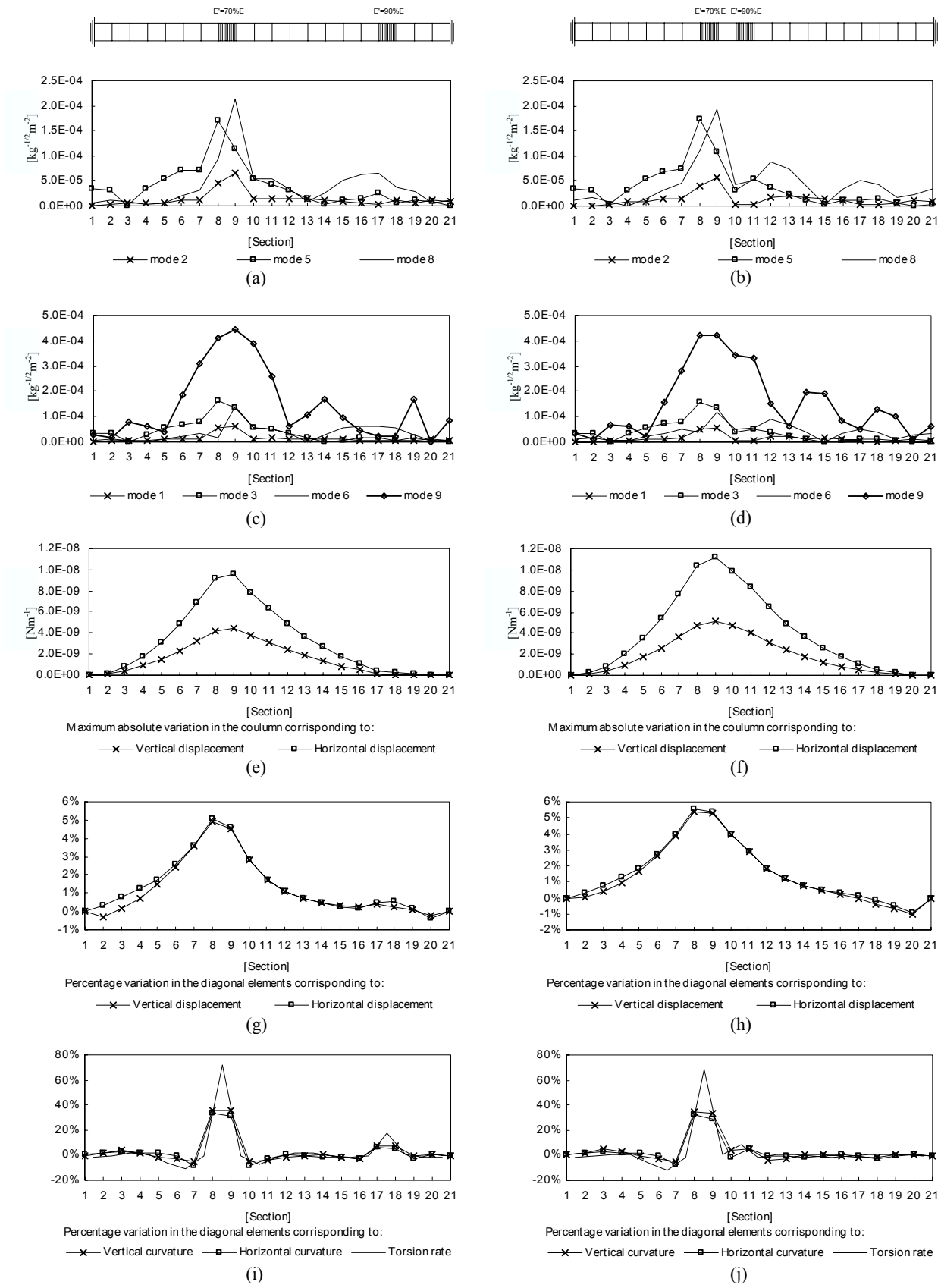

Figure 2: Damage indexes for damage scenarios D1 and D2: absolute changes in vertical modal curvature (a, b) and in horizontal modal curvature (c, d); maximum absolute changes in the flexibility matrix columns (e, f); percentage changes in the flexibility matrix diagonal elements (g, h); percentage changes in the strain-flexibility matrix diagonal elements (i, j).

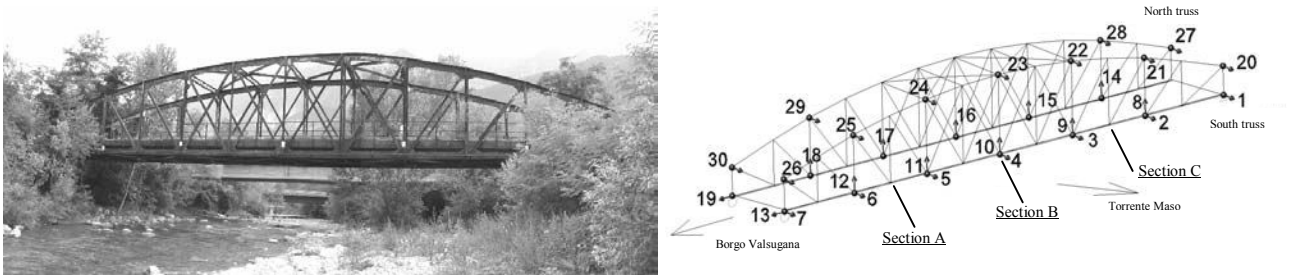

(a) (b)

Figure 3: (a) North view of the SP109 bridge during the experiment; (b) DOF considered in the dynamic characterization, with highlighted the three sections utilised for the graphical representation of Fig. 5.

Experimental application

The previously introduced damage location methods have been employed in the structural assessment of the SP109 bridge on the Maso run in Castelnuovo, near Trento, Italy. This bridge, originally built in 1894 and put out of service in 1974, is a 42.0 m long single-span steel structure consisting of two truss-beams supporting a 5.1 m wide deck (Fig. 4). Most of the structural elements are built-up, lattice or battened beams, and all the connections are made by hot riveting. Some elements of the two trusses show evidence of damage caused by impacts of vehicles. The position and the extension of this damage is summarized in Fig. 7(a). In addition, an advanced state of corrosion of the heads of the rivets has been observed at the lower chords of the two truss-beams.

Finite Element Model. A FE model has been utilised for reproducing the behaviour of the structure in the undamaged situation. Beam-type elements were used for modelling the truss and the brace system, while shell-type elements have been adopted for the slab. The mechanical properties of the material were evaluated through the analysis of 22 specimens, sampled at different points of the structure. The analysis of these specimens also allowed evaluating the average thickness of the rust layer as 0.4 mm; this information has been considered for defining the geometry of each beam element section. The model takes into account the equivalent shear flexibility of the trusses as well as the actual geometry of the nodes, including the eccentricities of the elements and the additional mass owed to the presence of rivets and connection plates. The actual mass of the 40 cm-thick slab has been detected through vertical cores, drilled at different points on the deck.

Dynamic characterization. The bridge was dynamically characterized by acquiring the structural response at 30 positions, as shown in Fig. 3(b), and performing shock tests in correspondence with two horizontal (4 and 5) and two vertical (10 and 11) Degrees of Freedom. The modal parameters were extracted using a Multi-Input-Multi-Output (MIMO) Curve Fitting method, which makes simultaneously use of the 4 sets of Frequency Response Functions in the optimisation process. The outcomes of the modal extraction are summarized in Fig. 5.

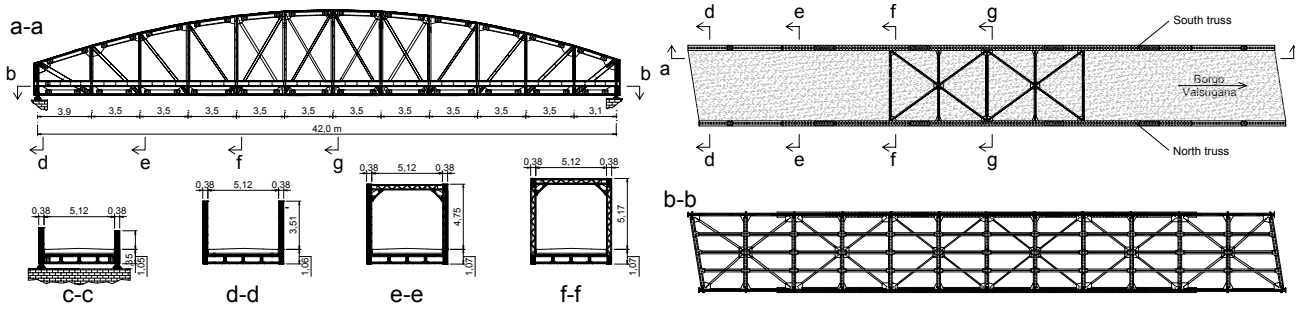

Figure 4: South truss, upper view, floor scheme and cross-sections of the SP109 bridge.

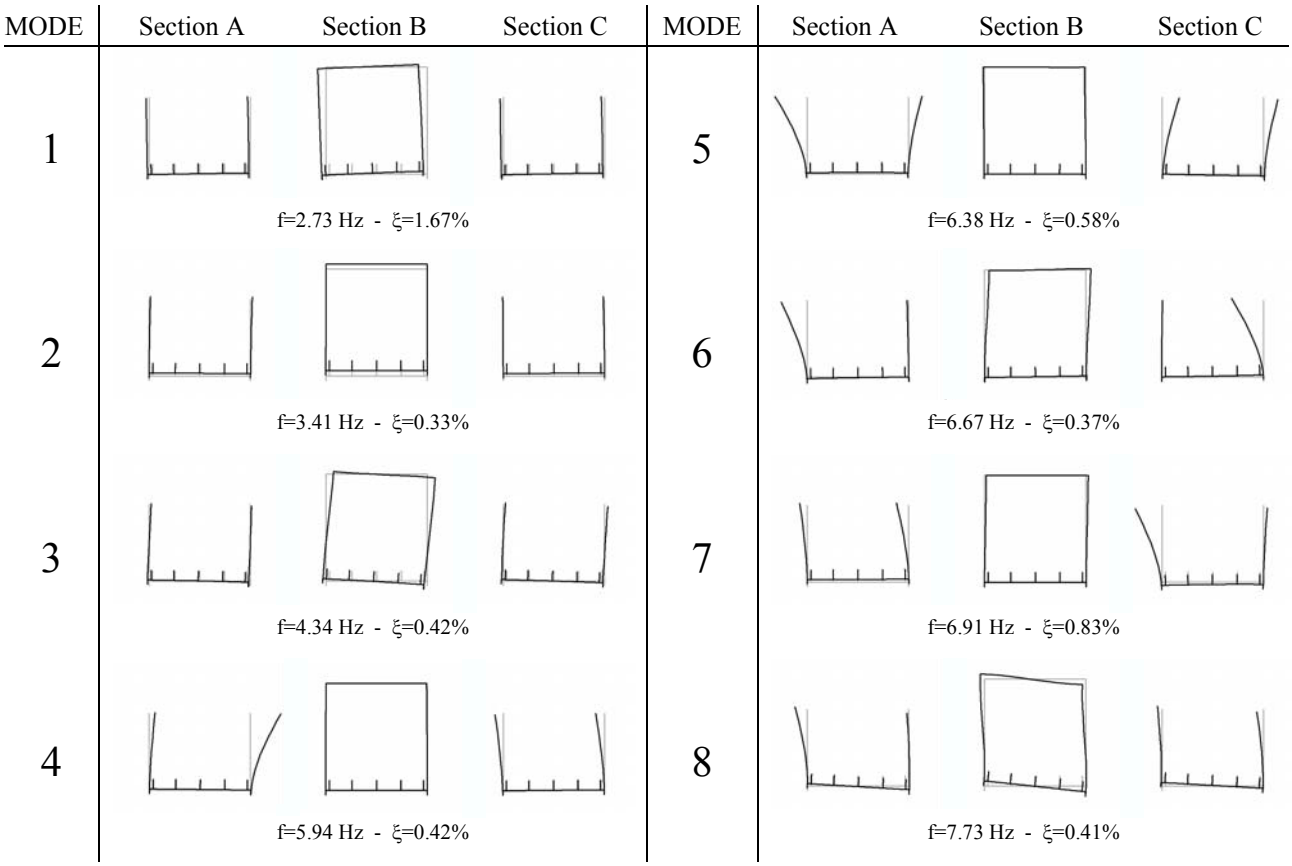

Figure 5: First eight experimental natural frequencies modal shapes and damping ratios of the SP109 bridge. Sections A, B and C are those represented in Fig. 3(b).

Damage location. With the scope of applying the different damage evaluation techniques, the bridge has been conceptually modelled as a beam-like structure, comprised of 7 independent sections, each endowed with 5 DoFs, as shown in Fig. 7(b). More specifically, the following section DoFs have been considered: the vertical displacement at the North truss, a_1; the vertical displacement at the South truss, a_2; the horizontal displacement of the slab, a_3; the slab rotation, θ; the section shear deformation at the North truss, α_N; the section shear deformation at the South truss α_S. Degrees of Freedom θ, α_N and α_S are related to the experimental measurements through the following expressions:

$$\theta = \frac{(a_2\text{-}a_1)}{b} \qquad \alpha_N = \frac{(a_3\text{-}a_5)}{H} \qquad \alpha_S = \frac{(a_3\text{-}a_4)}{H} \tag{5}$$

where b is the deck width and H is the truss-beam height, for each section.

Changes in the natural frequencies, mode shapes, strain mode shapes, flexibility matrix and strain-flexibility matrix have been considered in the location analysis. Methods based on changes in the natural frequencies and bare mode shapes did not provide information relevant to damage location. The flexibility matrix method allowed recognising in a qualitative manner the presence of damage, although it was not capable of providing precise information on its location and quantification.

Strain-mode-shapes based methods provided more precise information about location. However, only the analysis of the changes in the strain-flexibility matrix diagonal elements was capable of localising and quantifying the damage in few well-defined sections of the structure. The results of this analysis are graphically reported in Fig. 6.

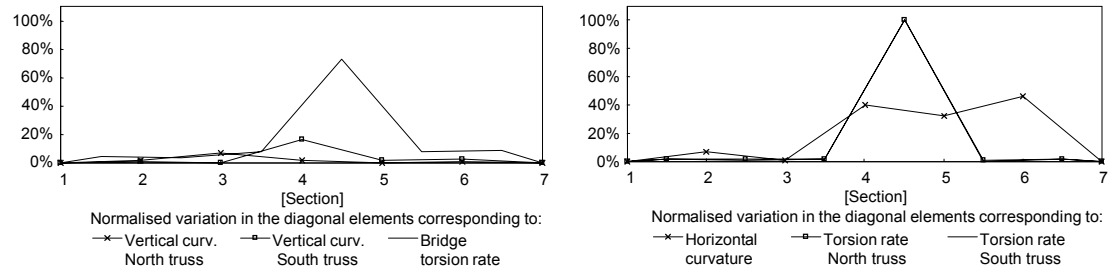

Figure 6: Changes in the strain-flexibility matrix diagonal elements for the SP109 bridge.

Discussion of the results. In order to utilize these outcomes for identifying potential damaged elements of the structure, a sensitivity FEM analysis has been conducted. This analysis allowed to correlating the theoretical outcomes of a strain-flexibility-based location with the simulated presence of damage in specific elements of the bridge, such as posts, web members and chords of the trusses, floor beams and brace system elements. Damaged elements pointed out by the sensitivity analysis include:

i) web members at the North truss about section 3;

ii) floor beams, top lateral and/or upper/lower diagonal elements between sections 4 and 5;

iii) quadrilaterals formed by the posts, the floor beam and the top lateral beam between sections 4 and 5;

iv) members of South truss about section 4.

The approximate location of these damaged areas is graphically represented in Fig. 7(a), compared with the actual position of damage evidenced by visual inspection (continuous line). It can be immediately recognised how areas (i), (ii) and (iii) actually include damage which are visually recognisable at the following elements: the post of the North truss (*a*), the top lateral and the upper diagonal at section 5 (*b* e *c*), the connection of the top lateral to the post at section 5 (*d*). The interpretation of the damage location at the South truss (iv) deserves a deeper consideration. The vertical curvature damage index shows the presence of a major damage at section 4 along with two lighter anomalies at sections 5 and 6. The latter can be easily correlated to damage *(f)* and (*g)* of Fig. 7(a). However, the high value of damage index found for section 4 highlights a significant loss in stiffness that cannot be explained with the sole presence of damage *(e)*. A static load test carried out on the bridge [9] showed that, for a symmetric load condition, the deflections measured at the South side are higher than those measured at the North side. This evidence indirectly confirms the significant loss in stiffness highlighted by the mode-shape-based damage evaluation. Reasonably, this should be due to the state of degradation that characterizes the lower chord of the truss at the middle-span, and that visual inspection can only partially reveal. Actually, visual inspections evidenced that parts the heads rivets are rusted in this zone, although it is not possible to estimate the influence of this disease on the overall behaviour of the structure.

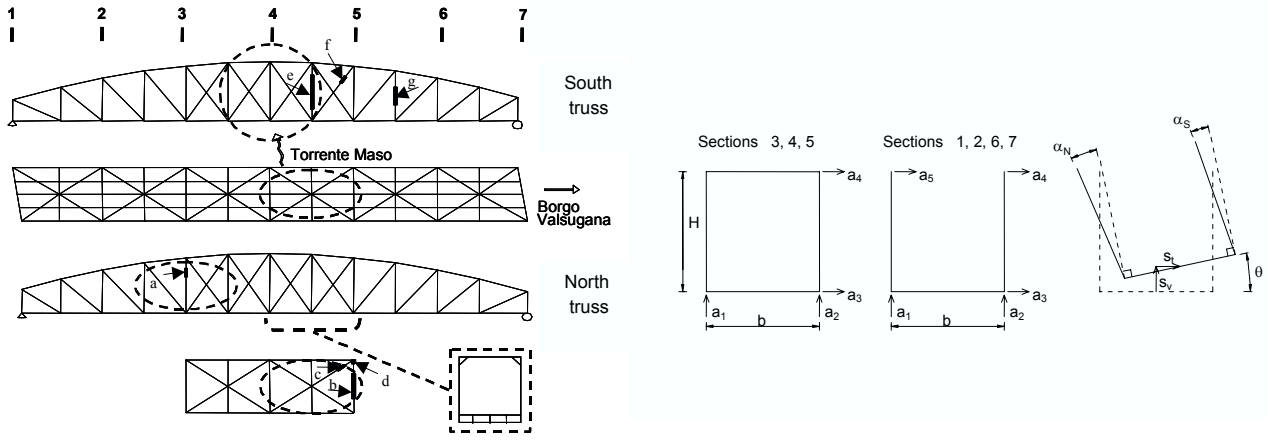

(a) (b)

Figure 7: (a) Damage location identified by non-destructive analysis (broken line) and by the visual inspection (bold line). (b) DoFs considered for each bridge section.

Summary

Different damage location approaches proposed in the literature have been compared and theoretically analysed. It has been observed that, when damage is modelled as a loss in stiffness, the most direct way of exploiting mode-shapes information is based on the estimation of the strain-flexibility matrix. The matrix can be easily computed starting from the measured natural frequencies and mode shapes expressed in terms of strain. Numerical examples showed that, even in the case of a statically indeterminate structure, the method is capable of resolving and quantifying multiple damages. Also, the application of this technique to the assessment of a real bridge allowed detecting a damage scenario, which is consistent with the visual evidence of damage and with the outcomes of a static load test.

Nevertheless, the experiment pointed out some issues concerning the practical application of these techniques to civil structures. Both the employment of a FEM for reproducing the behaviour of the undamaged structure, and the sensitivity of mode shape estimation to noise are sources of uncertainties. However, the main restriction to the precision of the method is related to the limited number of sensors that can be reasonably utilised in a test, with respect to the complexity of the investigated structure. In the reported case-study, the 30 measurement points employed in the dynamics characterization allowed for the calculation of curvature-based and torsion-rate-based damage indexes at sections 5 and 6 respectively, with a spatial resolution of 7 m only. In general, the huge number of sensors needed for obtaining an adequate spatial resolution in damage location represents today the main obstacle to a massive employment of mode-shape-based techniques in permanent monitoring, and justifies their application only to very specific classes of civil structures.

References

[1] S.W. Doebling, C.R. Farrar and M.B. Prime: *A summary review of vibration-based damage identification methods*, The Shock and Vibration Digest Vol. 30(2) (1998), pp. 91-105

[2] A.K. Pandey, M. Biswas and M.M. Samman: *Damage Detection from Changes in Curvature Mode Shapes*, J. of Sound and Vibration Vol. 145(2) (1991), pp. 321-332

[3] G.C. Yao, K.C. Chang and G.C. Lee: *Damage Diagnosis of Steel Frames Using Vibrational Signature Analysis,* J. of Engineering Mechanics Vol. 118(9) (1992), pp. 1949-1961

[4] J. Maeck and G. De Roeck: *Dynamic Bending and Torsion Stiffness Derivation from Modal Curvatures and Torsion Rate*, J. of Sound and Vibration Vol. 255(1) (1999), pp. 153-170

[5] N. Stubbs, J.T. Kim, C.R. Farrar: *Field Verification of a Nondestructive Damage Localization and Severity Estimation Algorithm*, (Proc. 13th International Modal Analysis Conference, Nashville, TN, USA, 1995), pp. 210-218

[6] A.K. Pandey and M. Biswas: *Damage Detection in Structures using Changes in Flexibility,* Journal of Sound and Vibration Vol. 169(1) (1994), pp. 3-17

[7] Q. Lu, G. Ren and Y. Zhao: *Multiple Damage Location with Flexibility Curvature and Relative Frequency Change for Beam Structures*, J. of Sound and Vibration Vol. 253(5) (2002), pp. 1101-1114

[8] D. Zonta, A.W. Elgamal, M. Fraser and M.J.N. Priestly: *A Vibrational Based Methodology For After-Earthquake Damage Assessment Of Multistory Frame-Resistant Buildings,* (Proc. 12th European Conf. on Earthquake Engineering, London, 2002)

[9] P. Prada: *Indagine Teorico-sperimentale su un Ponte Metallico con Unioni Chiodate del XIX Secolo: Studio del Comportamento Statico*, (Laurea Thesis, DIMS, University of Trento, 2002)